Three-body decays $B \to \phi(\rho)K\gamma$ in perturbative QCD approach

Chao Wang,[1,*] Jing-Bin Liu,[1,†] Hsiang-nan Li,[2,‡] and Cai-Dian Lü[1,§]
[1]Institute of High Energy Physics, CAS, P.O. Box 918, Beijing 100049, China
and University of Chinese Academy of Sciences, Beijing 100049, China
[2]Institute of Physics, Academia Sinica, Taipei, Taiwan 115, Republic of China

(Received 24 December 2017; published 27 February 2018)

We study the three-body radiative decays $B \to \phi(\rho)K\gamma$ induced by a flavor-changing neutral current in the perturbative QCD approach. Pseudoscalar-vector (PV) distribution amplitudes (DAs) are introduced for the final-state ϕK (ρK) pair to capture important infrared dynamics in the region with a small PV-pair invariant mass. The dependence of these PV DAs on the parton momentum fraction is parametrized in terms of the Gegenbauer polynomials, and the dependence on the meson momentum fraction is derived through their normalizations to timelike PV form factors. In addition to the dominant electromagnetic penguin, the subleading chromomagnetic penguin, quark-loop and annihilation diagrams are also calculated. After determining the PV DAs from relevant branching-ratio data, the direct CP asymmetries and decay spectra in the PV-pair invariant mass are predicted for each $B \to \phi(\rho)K\gamma$ mode.

DOI: 10.1103/PhysRevD.97.034033

I. INTRODUCTION

A large number of experimental investigations on three-body hadronic B meson decays have been carried out by the *BABAR* [1–6], Belle [7–10] and LHCb [11–13] Collaborations in recent decades. The forthcoming Belle-II experiments will further improve the accuracy of their measurements by means of Dalitz analyses [14]. These decays, involving QCD dynamics much more complicated than in two-body ones, impose a severe challenge to the development of corresponding theoretical frameworks. The currently available frameworks based on the factorization theorem for three-body hadronic B meson decays include the perturbative QCD (PQCD) approach [15–18] and the QCD-improved factorization approach [19–21]. Though the factorization theorem is not yet proved rigorously, phenomenological applications have been attempted, and abundant predictions have been made. There exist other approaches, such as final state interactions [22] and heavy meson chiral perturbation theory [23,24]. The stringent confrontation of theoretical predictions with data in the whole final state phase space is likely to reveal new dynamics, signifying the importance of three-body hadronic B meson decays.

Most of PQCD studies of the above decays focus on the kinematic configuration corresponding to edges of a Dalitz plot, whose formalism can be simplified by the introduction of two-hadron distribution amplitudes (DAs) [15]. In these regions two of the three final state hadrons collimate with each other in the rest frame of the B meson. At the quark level this configuration involves the hadronization of two energetic collinear quarks, produced from the b quark decay, into the two collimated hadrons. The hadron-pair system, dominated by infrared QCD dynamics, can then be factorized out of the whole process, and defines the two-hadron DA $\Phi_{h_1h_2}$ [25–28]. The factorization formula for the $B \to h_1h_2h_3$ decay is then expressed as

$$\mathcal{M} = \Phi_B \otimes H \otimes \Phi_{h_1h_2} \otimes \Phi_{h_3}, \tag{1}$$

where Φ_B (Φ_{h_3}) denotes the B meson (h_3 hadron) DA, and $\otimes$ means the convolution in parton momenta. The hard kernel H for the b quark decay, similar to the two-body case, starts with the diagrams of single hard gluon exchange. An advantage of the above formalism is that both resonant and nonresonant contributions to the hadron-pair system can be included into the two-hadron DA through appropriate parametrization. Although Eq. (1) has been applied to the whole three-body phase space, it should be understood that it is precise only in the region with a small hadron-pair invariant mass. A two-hadron DA loses its accuracy in the central region of a Dalitz plot, where the major contribution to three-body decays arises from two hard gluon exchanges [15]. Nevertheless, it is also

*wangchao88@ihep.ac.cn
†liujb@ihep.ac.cn
‡hnli@phys.sinica.edu.tw
§lucd@ihep.ac.cn

the region, where a two-hadron DA decreases with certain power law of the invariant mass, and gives a minor contribution.

In this paper we will extend the PQCD approach to the three-body radiative decays $B \to PV\gamma$ with P (V) representing a pseudoscalar (vector) meson. The significance of these decays has been well recognized: the involved flavor-changing neutral current $b \to s\gamma$, occurring only at loop level in the standard model, is sensitive to new physics effects. Following the similar reasoning, the two-hadron DAs Φ_{PV} can be introduced to collect the dominant contribution from the region with a small PV-pair invariant mass m_{PV}. For instance, nearly 72% of the signal events appear in the low mass region with $m_{\phi K} \in [1.5, 2.0]$ GeV [29]. Besides, the emitted photons from the leading electromagnetic $O_{7\gamma}$ transition are mainly left-handed (right-handed) in B^- and $\bar{B}^0$ (B^+ and B^0) meson decays. A chirality flip may be induced by local four-quark operators and the chromomagnetic penguin operator O_{8g} from QCD corrections, as well as by final state interactions among various resonant channels [30]. We will address the above subjects, taking the $B \to \phi(\rho)K\gamma$ decays as examples. The resonant contribution to the ϕK system is negligible [29,31], so the parametrization for the DAs $\Phi_{\phi K}$ in Ref. [32], which contain timelike form factors with certain power-law behavior, is adopted. The resonant contributions from the states $K_1(1270)$ and $K^*(1680)$ to the ρK system dominate [33,34]. Therefore, the parametrization of the DAs $\Phi_{\rho K}$ follows that for quasi-two-body B meson decays [17,18,35,36], namely, the Breit-Wigner model.

In Sec. II we construct the PV DAs according to the procedure proposed in [32]: the dependence on the parton momentum fraction is parametrized in terms of the Gegenbauer polynomials, and the dependence on the meson momentum fraction is derived through their normalizations to time-like PV form factors. In Sec. III we analyze the three-body radiative decays $B \to \phi(\rho)K\gamma$, determine the PV DAs from relevant branching-ratio data, and then predict their direct CP asymmetries, photon polarization asymmetries, and decay spectra in the PV-pair invariant mass. Our work is more complete than [32], because the contributions from the operators $O_{7\gamma}$, O_{8g}, and O_2 are all considered, and the annihilation diagrams are calculated. The summary is given in the last section, and the factorization formulas for the $B \to \phi(\rho)K\gamma$ decay amplitudes are collected in the Appendix.

II. PSEUDOSCALAR-VECTOR DISTRIBUTION AMPLITUDES

We choose the B meson momentum P_B, the PV-pair momentum P, and the photon momentum P_γ in the light-cone coordinates as

$$P_B = \frac{m_B}{\sqrt{2}}(1,1,\mathbf{0}_T), \qquad P = \frac{m_B}{\sqrt{2}}(1,\eta,\mathbf{0}_T),$$
$$P_\gamma = \frac{m_B}{\sqrt{2}}(0,1-\eta,\mathbf{0}_T), \tag{2}$$

with the B meson mass m_B and the variable $\eta = P^2/m_B^2 \equiv \omega^2/m_B^2$, ω being the invariant mass of the PV pair. Define the momenta of the vector and pseudoscalar mesons by

$$P_1 = (\zeta P^+, [(1-\zeta)\eta + r_V^2]P^+, \sqrt{(\zeta\omega^2 - m_V^2)(1-\zeta)}, 0),$$
$$P_2 = ((1-\zeta)P^+, (\zeta\eta - r_V^2)P^+, -\sqrt{(\zeta\omega^2 - m_V^2)(1-\zeta)}, 0), \tag{3}$$

respectively, which obey $P = P_1 + P_2$, with the vector meson momentum fraction ζ and the mass ratio $r_V = m_V/m_B$. The smaller pseudoscalar mass has been neglected. Write the spectator momenta in the B meson and in the PV pair as

$$k_1 = \left(0, \frac{m_B}{\sqrt{2}}x_1, \boldsymbol{k}_{1T}\right), \qquad k_2 = \left(\frac{m_B}{\sqrt{2}}z, 0, \boldsymbol{k}_{2T}\right), \tag{4}$$

respectively, x_1 and z being the momentum fractions. We also define the polarization vectors ϵ of the PV system by

$$\epsilon^*(\pm) = \frac{1}{\sqrt{2}}(0,0,\mp 1,-i), \quad \epsilon_L^* = \frac{1}{\sqrt{2\eta}}(1,-\eta,\mathbf{0}_T). \tag{5}$$

A two-meson DA $\phi(z,\zeta,\omega)$ describes the hadronization of two collinear quarks, together with other quarks popped out of the vacuum and playing no role in a hard decay process, into two collimated mesons. It can be decomposed in terms of the eigenfunctions of the ERBL evolution equation [37,38], i.e., the Gegenbauer polynomials $C_n^{3/2}(2z-1)$, and the partial waves, i.e., the Legendre polynomials $P_l(2\zeta - 1)$ [26,28]. However, for the PV system, the different spins of the pseudosalar and the vector render the Legendre polynomial expansion not applicable. Hence, we extract the ζ dependence from the normalizations of the PV DAs to the associated timelike form factors [32], which depend on the PV-pair invariant mass ω, a procedure similar to deriving the two-pion DAs via the process $\gamma\gamma^* \to \pi^+\pi^-$ [39]. To be explicit, we evaluate perturbatively the matrix elements of local currents

$$\langle V(P_1, \epsilon^*(V))P(P_2)|\bar{q}'(0)\Gamma q(0)|0\rangle, \tag{6}$$

using the vector and pseudoscalar DAs up to twist 3, where the polarization vectors of the vector meson satisfy $\epsilon^*(V)\cdot P_1 = 0$ and $\epsilon^*(V)^2 = -1$, and Γ represents the possible spin projectors I, γ_5, γ_μ, $\gamma_\mu\gamma_5$, and $\sigma_{\mu\nu}\gamma_5$. The above matrix element is precisely the normalization of the

PV DA associated with the spin projector Γ, and also the PV timelike form factor associated with the local current $\bar{q}'\Gamma q$. The objective of the perturbative calculation is to identify the kinematic structure of the matrix element in terms of P_1, $\epsilon^*(V)$, and P_2 for each Γ, which are then approximated by the momentum P and the polarization vectors ϵ^* of the PV system according to the power counting rules in the heavy quark limit [32]. In this way we obtain the ζ dependence of the PV DAs up to twist 3, i.e., $\mathcal{O}(\omega/m_B)$.

The expansions of the nonlocal matrix elements for various spin projectors Γ up to twist 3 are listed below:

$$\begin{aligned}&\langle PV|\bar{q}'(y^-)\gamma_\mu\gamma_5 q(0)|0\rangle\\&= P_\mu\int_0^1 dz e^{izP\cdot y}\phi_\parallel(z,\zeta,\omega)+\omega\epsilon^*_{T\mu}\\&\quad\times\int_0^1 dz e^{izP\cdot y}\phi_a(z,\zeta,\omega),\end{aligned}\tag{7}$$

$$\begin{aligned}&\langle PV|\bar{q}'(y^-)\sigma_{\mu\nu}\gamma_5 q(0)|0\rangle\\&= -i\Big\{(\epsilon^*_{T\mu}P_\nu-\epsilon^*_{T\nu}P_\mu)\int_0^1 dz e^{izP\cdot y}\phi_T(z,\zeta,\omega)\\&\quad+(\epsilon^*_{L\mu}P_\nu-\epsilon^*_{L\nu}P_\mu)\int_0^1 dz e^{izP\cdot y}\phi_3(z,\zeta,\omega)\Big\},\end{aligned}\tag{8}$$

$$\langle PV|\bar{q}'(y^-)\gamma_5 q(0)|0\rangle=\omega\int_0^1 e^{izP\cdot y}\phi_p(z,\zeta,\omega),\tag{9}$$

$$\begin{aligned}&\langle PV|\bar{q}'(y^-)\gamma_\mu q(0)|0\rangle\\&= i\frac{\omega}{P\cdot n_-}\epsilon_{\mu\nu\rho\sigma}\epsilon_T^{*\nu}P^\rho n_-^\sigma\int_0^1 e^{izP\cdot y}\phi_v(z,\zeta,\omega),\end{aligned}\tag{10}$$

$$\langle PV|\bar{q}'(y^-)Is(0)|0\rangle=0,\tag{11}$$

where $n_-=(0,1,\mathbf{0}_T)$ is a lightlike vector, the convention $\epsilon_{0123}=-1$ has been employed, and the PV DAs $\phi_{\parallel,t}$ ($\phi_{p,3,a,v}$) are of twist 2 (twist 3). To get the first term in Eq. (7), we have applied

$$(P_1-P_2)_\mu\simeq(2\zeta-1)P_\mu,\tag{12}$$

in which the coefficient $2\zeta-1$ is absorbed into the DA $\phi_\parallel$, giving rise to its ζ dependence. We have also made the approximation

$$\epsilon^*_{T\mu}(V)P_{1\nu}-\epsilon^*_{T\nu}(V)P_{1\mu}\simeq\zeta(\epsilon^*_{T\mu}P_\nu-\epsilon^*_{T\nu}P_\mu),\tag{13}$$

$$\frac{2}{\omega}(P_{1\mu}P_{2\nu}-P_{1\nu}P_{2\mu})\simeq(2\zeta-1)(\epsilon^*_{L\mu}P_\nu-\epsilon^*_{L\nu}P_\mu),\tag{14}$$

as arriving at Eq. (8). It is found, compared to [32], that the term $(P_{1\mu}P_{2\nu}-P_{1\nu}P_{2\mu})$ does not generate the twist-2 contribution $(\epsilon_{T\mu}P_\nu-\epsilon_{T\nu}P_\mu)$, since a transverse momentum and a transverse polarization have different physical meanings. Equation (10) comes from the approximation of the kinematic factor

$$\frac{2}{\omega}\epsilon_{\mu\nu\rho\sigma}\epsilon_T^{*\nu}(V)p_1^\rho p_2^\sigma\simeq\frac{\omega}{P\cdot n_-}(2\zeta-1)\epsilon_{\mu\nu\rho\sigma}\epsilon_T^{*\nu}P^\rho n_-^\sigma.\tag{15}$$

We summarize the PV DAs for the longitudinal and transverse polarizations from Eqs. (7)–(11) as

$$\begin{aligned}\langle PV(P,\epsilon_L^*)|\bar{q}'(y^-)_j q(0)_l|0\rangle&=\frac{1}{\sqrt{2N_c}}\int_0^1 dz e^{izP\cdot y}\{(\gamma_5\not{P})_{lj}\phi_\parallel(z,\zeta,\omega)+(\gamma_5)_{lj}\omega\phi_p(z,\zeta,\omega)+(\gamma_5\not{\epsilon}^*_L\not{P})_{lj}\phi_3(z,\zeta,\omega)\},\\\langle PV(P,\epsilon_T^*)|\bar{q}'(y^-)_j q(0)_l|0\rangle&=\frac{1}{\sqrt{2N_c}}\int_0^1 dz e^{izP\cdot y}\{(\gamma_5\not{\epsilon}^*_T\not{P})_{lj}\phi_t(z,\zeta,\omega)+(\gamma_5\not{\epsilon}^*_{T\mu})_{lj}\omega\phi_a(z,\zeta,\omega)\\&\quad+i\frac{\omega}{P\cdot n_-}\epsilon_{\mu\nu\rho\sigma}(\gamma^\mu)_{lj}\epsilon_T^{*\nu}P^\rho n_-^\sigma\phi_v(z,\zeta,\omega)\}.\end{aligned}\tag{16}$$

They contain the products of the timelike form factors $F(\omega)$, which define the normalizations of the DAs, and the z-dependent and ζ-dependent functions:

$$\begin{aligned}&\phi_\parallel(z,\zeta,\omega)=\frac{3F_\parallel(\omega)}{\sqrt{2N_c}}f_\parallel(z)(2\zeta-1),\quad\phi_p(z,\zeta,\omega)=\frac{3F_p(\omega)}{\sqrt{2N_c}}f_p(z),\quad\phi_3(z,\zeta,\omega)=\frac{3F_3(\omega)}{\sqrt{2N_c}}f_3(z)(2\zeta-1),\\&\phi_t(z,\zeta,\omega)=\frac{3F_T(\omega)}{\sqrt{2N_c}}f_t(z)\zeta,\quad\phi_a(z,\zeta,\omega)=\frac{3F_a(\omega)}{\sqrt{2N_c}}f_a(z),\quad\phi_v(z,\zeta,\omega)=\frac{3F_v(\omega)}{\sqrt{2N_c}}f_v(z)(2\zeta-1).\end{aligned}\tag{17}$$

Different from Ref. [32], the DA ϕ_a in the above expressions does not depend on the meson momentum fraction ζ. Note that only the DAs for the transversely polarized PV pair are relevant to the three-body radiative decays $B\to PV\gamma$ considered here.

We include the first Gegenbauer moment for the function $f_a(z)$, making the ϕK DA ϕ_a a bit asymmetric in the parton momentum distribution, and assume the asymptotic form $z(1-z)$ for the functions $f_{t,v}(z)$ for simplicity,

$$\begin{aligned}\phi_t(z,\zeta,\omega) &= \frac{3F_T^{\phi K}(\omega)}{\sqrt{2N_c}} z(1-z)\zeta,\\ \phi_a(z,\zeta,\omega) &= \frac{3F_a^{\phi K}(\omega)}{\sqrt{2N_c}} z(1-z)[1+a_1 C_1^{3/2}(2z-1)],\\ \phi_v(z,\zeta,\omega) &= \frac{3F_v^{\phi K}(\omega)}{\sqrt{2N_c}} z(1-z)(2\zeta-1).\end{aligned} \tag{18}$$

The ϕK timelike form factors, dominated by nonresonant contributions, are parametrized as [32]

$$\begin{aligned}F_T^{\phi K}(\omega) &= \frac{m_T^2}{(\omega-m_l)^2+m_T^2},\\ F_a^{\phi K}(\omega) = F_v^{\phi K}(\omega) &= \frac{m_0 m_\parallel^2}{(\omega-m_l)^3+m_0 m_\parallel^2},\end{aligned} \tag{19}$$

with the chiral scale $m_0 \simeq 1.7$ GeV [40] and the threshold invariant mass $m_l = m_\phi + m_K$. That is, we keep the pseudoscalar mass only in the phase space allowed for the time-like form factors. The tunable parameters a_1 and $m_T \simeq m_\parallel$, expected to be few GeV, will be determined from the fit to the data of the $B \to \phi K\gamma$ branching ratios. Since ϕ_a gives a larger contribution, as verified numerically in the next section, the data lead stronger constraint to its first Gegenbauer moment. This explains why we introduce a_1 only into ϕ_a.

The amplitude analysis on the resonant structure of the final state in the $B^+ \to K^+\pi^-\pi^+\gamma$ decay [34] provides a useful guideline for parametrizing the resonant contribution to the $B \to \rho K\gamma$ mode, for which $K_1(1270)$ and $K^*(1680)$ are the major intermediate resonances. The resonance $K_1(1270)$ is a mixture of the $K_{1A}(1^3P_1)$ and $K_{1B}(1^1P_1)$ states,

$$\begin{aligned}K_1(1270) &= \sin\theta_K K_{1A} + \cos\theta_K K_{1B},\\ K_1(1400) &= \cos\theta_K K_{1A} - \sin\theta_K K_{1B},\end{aligned} \tag{20}$$

θ_K being the mixing angle. With the insertion of Eq. (20), the quasi-two-body $B \to K_1(1270)(\to \rho K)\gamma$ decay amplitude can be expressed as the combination of the $B \to K_{1A}(\to \rho K)\gamma$ amplitude and the $B \to K_{1B}(\to \rho K)\gamma$ amplitude, such that the K_{1A} and K_{1B} meson DAs with the specific symmetry in the z dependence can be employed. The ρK DAs for the $B \to K_1(1270)(\to \rho K)\gamma$ modes are then parametrized as

$$\begin{aligned}\phi_t(z,\zeta,\omega) &= \frac{3F_1^{\rho K}(\omega)}{\sqrt{2N_c}} c_K z(1-z)\Big[a_0^\perp + 3a_1^\perp(2z-1)\\ &\quad + a_2^\perp\frac{3}{2}(5(2z-1)^2-1)\Big]\zeta,\\ \phi_a(z,\zeta,\omega) &= \frac{F_1^{\rho K}(\omega)}{2\sqrt{2N_c}} c_K\Big[\frac{3}{4}a_0^\parallel(1+(2z-1)^2)\\ &\quad + \frac{3}{2}a_1^\parallel(2z-1)^3\Big],\\ \phi_v(z,\zeta,\omega) &= \frac{3F_1^{\rho K}(\omega)}{4\sqrt{2N_c}} c_K[a_0^\parallel(1-2z)\\ &\quad + a_1^\parallel(6z-6z^2-1)](2\zeta-1),\end{aligned} \tag{21}$$

where the mixing factor c_K and the Gegenbauer moments associated with the $K_{1A}(K_{1B})$ state take the values

$$\begin{aligned}&c_K = \sin\theta_K(\cos\theta_K), \qquad a_0^\parallel = 1(-0.15\pm0.15),\\ &a_1^\parallel = -0.30^{+0.26}_{-0.00}(-1.95+0.45), \qquad a_0^\perp = 0.26^{+0.03}_{-0.22}(1),\\ &a_1^\perp = -1.08\pm0.48(0.30^{+0.00}_{-0.31}),\\ &a_2^\perp = 0.02\pm0.21(-0.02\pm0.22).\end{aligned} \tag{22}$$

In principle, the Gegenbauer moments for the ρK DAs are free parameters. Here we adopt those for the K_{1A} and K_{1B} DAs [41,42] as their typical values in the numerical study below. The form factor $F_1^{\rho K}$ picks up the standard Breit-Winger model,

$$F_1^{\rho K}(\omega) = \frac{m_{K_1(1270)}^2}{m_{K_1(1270)}^2 - \omega^2 - i m_{K_1(1270)}\Gamma_{K_1(1270)}}, \tag{23}$$

$m_{K_1(1270)}$ ($\Gamma_{K_1(1270)}$) being the mass (decay width) of the $K_1(1270)$ meson.

Note that we have proposed different parametrizations of the nonresonant and resonant contributions: for the former, the final state interaction is ignored, and their form factors are real and normalized to $F(m_l) = 1$. Because it arises from a wider range of the invariant mass, the different power-law behaviors of the form factors, $F_T^{\phi K} \sim 1/\omega^2$ and $F_{a,v}^{\phi K}(\omega) \sim m_0/\omega^3$ at large ω [43–45], have been taken into account. For the latter, the major contribution comes from the region around the resonance mass, so it is reasonable not to differentiate the power-law behaviors of the form factors in $\phi_{t,a,v}$, but parametrize them in terms of the same Breit-Wigner model.

Another resonance $K^*(1680)$ contributes via the $B \to K^*(1680)(\to \rho K)\gamma$ channel [33,34]. Since the Gegenbauer moments of the $K^*(1680)$ DAs are unknown, we simply assume the asymptotic form $z(1-z)$ for the z dependence of the corresponding ρK DAs. The standard Breit-Wigner model is also used for the associated form factor

$$F_2^{\rho K}(\omega) = \frac{c m_{K^*(1680)}^2}{m_{K^*(1680)}^2 - \omega^2 - i m_{K^*(1680)}\Gamma_{K^*(1680)}}, \quad (24)$$

where the parameter c, characterizing the strength relative to the amplitude from the resonance $K_1(1270)$, will be determined from the fit to the measured $B \to \rho K\gamma$ branching ratios. There is no interference between the K_1 and K^* states because of their different quantum numbers. Denoting the amplitude from the $K_1(1270)$ ($K^*(1680)$) channel by $\mathcal{A}_1$ ($\mathcal{A}_2$), we compute the total amplitude squared for the $B \to \rho K\gamma$ decays according to [34]

$$|\mathcal{A}|^2 = \frac{1}{1+c^2}[|\mathcal{A}_1|^2 + |\mathcal{A}_2|^2], \quad (25)$$

in which the factor $1/(1+c^2)$ plays the role of an overall normalization.

III. NUMERICAL RESULTS

As stated before, the evaluation of the three-body radiative B meson decay amplitudes reduces to that of two-body ones [46–48] with the introduction of the PV DAs. We consider the $O_{7\gamma}$, O_{8g}, and O_2 operators, and the annihilation contributions, performing an analysis more complete than in [32], where only the emission diagrams from $O_{7\gamma}$ were included. The explicit factorization formulas for various contributions are collected in the Appendix. The $B \to PV\gamma$ differential decay rate, i.e., the decay spectrum in the PV invariant mass, is then derived from

$$\frac{d\Gamma}{d\omega} = \frac{1}{128\pi^3}\sqrt{\eta}(1-\eta)\int_{m_l^2/\omega^2}^1 d\zeta(|\mathcal{A}^R|^2 + |\mathcal{A}^L|^2), \quad (26)$$

where the vector meson momentum fraction ζ is bounded by $m_l^2/\omega^2 \le \zeta \le 1$, and $\mathcal{A}^{R(L)}$ represents the amplitude for the right-handed (left-handed) photon emission.

The inputs for the masses (in units of GeV) [49], the widths of the K_1 and K^* mesons (in units of GeV) [34], and the mean lifetimes of the B mesons (in units of ps) are listed below:

$$\begin{aligned} m_{B^{\pm,0}} &= 5.280, & m_\phi &= 1.019, \\ m_{K^\pm} &= 0.494, & m_{K^0} &= 0.498, \\ m_\rho &= 0.775, & m_{K_1(1270)} &= 1.272, \\ m_{K^*(1680)} &= 1.717, & \Gamma_{K_1(1270)} &= 0.098, \\ \Gamma_{K^*(1680)} &= 0.377, & \tau_{B^\pm} &= 1.638, \\ \tau_{B^0} &= 1.519. \end{aligned} \quad (27)$$

Phenomenological investigations in the literature and experimental data have indicated that the mixing angle θ_K for the K_{1A} and K_{1B} mesons is around either 33° or 58° [50–56]. As to the Cabibbo-Kobayashi-Maskawa (CKM) matrix elements, we employ the Wolfenstein parametrization with the inputs [49],

$$\lambda = 0.222506 \pm 0.00050, \qquad A = 0.811 \pm 0.026,$$
$$\bar\rho = 0.124^{+0.019}_{-0.018}, \qquad \bar\eta = 0.356 \pm 0.011.$$

In addition, we take the B meson decay constant $f_B = 0.190$ GeV, which is in agreement with the lattice results $f_B = 0.186 \pm 0.004$ GeV [57] and $f_B = 0.186 \pm 0.013$ GeV [58], and with those from the recent theoretical studies [59,60].

We take into account the following theoretical uncertainties. The first source of errors originates from the hadronic parameters, specifically the shape parameter of the B meson DA, $\omega_B = 0.40 \pm 0.04$ GeV. For the $B \to \rho K\gamma$ decays, this source of errors also includes the variation of the Gegenbauer moments in the ρK DAs. The second source characterizes the next-to-leading-order effects in the PQCD approach: we vary the hard scale t from $0.80t$ to $1.2t$ (without changing $1/b_i$) and the QCD scale $\Lambda_{\rm QCD} = 0.25 \pm 0.05$ GeV. The CKM matrix elements V_{tb} and V_{ts} involved in the dominant operator $O_{7\gamma}$ have small uncertainties, so the resultant error will be ignored in our numerical analysis.

The Gegenbauer moment a_1 in Eq. (18) and the free parameters $m_{T,\parallel}$ in Eq. (19) can be extracted from the branching-ratio data [49]

$$\begin{aligned} \mathcal{B}_{\rm exp}(B^+ \to \phi K^+\gamma) &= (2.7 \pm 0.4) \times 10^{-6}, \\ \mathcal{B}_{\rm exp}(B^0 \to \phi K^0\gamma) &= (2.7 \pm 0.7) \times 10^{-6}. \end{aligned} \quad (28)$$

We obtain for $a_1 = -0.3$ and $m_{T,\parallel} = 3.0$ GeV,

$$\begin{aligned} \mathcal{B}(B^+ \to \phi K^+\gamma) &= (2.69^{+0.18+0.43}_{-0.18-0.36}) \times 10^{-6}, \\ \mathcal{B}(B^0 \to \phi K^0\gamma) &= (2.41^{+0.14+0.37}_{-0.18-0.35}) \times 10^{-6}, \end{aligned} \quad (29)$$

which match the observed values well. The negative a_1 implies that the light spectator quark intends to carry, as expected, a smaller fraction of the ϕK pair momentum. It has been examined that the above results are stable against the variation of $m_{T,\parallel}$ around few GeV. The central value of $\mathcal{B}(B^+ \to \phi K^+\gamma)$ in Eq. (29) is lower than the prediction $(2.9^{+0.7}_{-0.5}) \times 10^{-6}$ in [32] because of the combined effects of the following changes: retaining the kaon mass here suppresses the phase space, but the asymmetric DA ϕ_a compensates the reduction a bit.

The exclusive B meson decays into the resonances $K_1(1270)$ and $K^*(1680)$ have been reported by *BABAR* with the branching ratios [34],

$$\begin{aligned} \mathcal{B}_{\rm exp}(B^+ \to K_1(1270)^+\gamma) &= (44.1^{+8.6}_{-7.3}) \times 10^{-6}, \\ \mathcal{B}_{\rm exp}(B^+ \to K^*(1680)^+\gamma) &= (66.7^{+17.1}_{-13.8}) \times 10^{-6}. \end{aligned} \quad (30)$$

The branching factions of the $K_1(1270)$ and $K^*(1680)$ transitions into the ρK final state [49]

$$\mathcal{B}_{\rm exp}(K_1(1270)\to\rho K)=(42\pm6)\%,$$
$$\mathcal{B}_{\rm exp}(K^*(1680)\to\rho K)=(31.4^{+5.0}_{-2.1})\%, \quad (31)$$

then lead to

$$\mathcal{B}_{\rm exp}(B^+\to K_1(1270)^+(\to\rho^0K^+)\gamma)=(6.2^{+1.5}_{-1.3})\times10^{-6}, \quad (32)$$

$$\mathcal{B}_{\rm exp}(B^+\to K^*(1680)^+(\to\rho^0K^+)\gamma)=(7.0^{+2.1}_{-1.5})\times10^{-6}. \quad (33)$$

Note that the total branching ratio [34]

$$\mathcal{B}_{\rm exp}(B^+\to\rho^0K^+\gamma)=(8.2\pm0.9)\times10^{-6}, \quad (34)$$

deviates from the sum of Eqs. (32) and (33), since the nonresonant contribution and the other minor $K_1(1400)$, $K^*(1410)$, and $K_2^*(1430)$ resonant contributions, which may cause destructive interference, have been neglected. The free parameter c in Eq. (24), characterizing the magnitude of the $K^*(1680)$ resonant contribution relative to the $K_1(1270)$ one, is determined by the fit to Eqs. (32) and (33). Note that the parameter c has reflected the strength of the $K^*(1680)\to\rho K$ transition.

For $\theta_K=33°$, the best fit value $c=2.0$ yields

$$\mathcal{B}(B^+\to K_1(1270^+)(\to\rho^0K^+)\gamma)=6.11^{+1.94+0.83}_{-1.44-1.40}\times10^{-6},$$
$$\mathcal{B}(B^+\to K^*(1680^+)(\to\rho^0K^+)\gamma)=6.72^{+2.12+1.03}_{-1.63-1.41}\times10^{-6}, \quad (35)$$

and the branching ratios of the B^0 meson decays are predicted to be

$$\mathcal{B}(B^0\to K_1(1270^0)(\to\rho^0K^0)\gamma)=5.00^{+1.71+0.73}_{-1.27-1.21}\times10^{-6},$$
$$\mathcal{B}(B^0\to K^*(1680^0)(\to\rho^0K^0)\gamma)=6.13^{+1.96+0.99}_{-1.53-1.32}\times10^{-6}. \quad (36)$$

For $\theta_K=58°$, we choose the best fit value $c=1.8$, obtaining

$$\mathcal{B}(B^+\to K_1(1270^+)(\to\rho^0K^+)\gamma)=5.95^{+1.92+0.75}_{-1.43-1.26}\times10^{-6},$$
$$\mathcal{B}(B^+\to K^*(1680^+)(\to\rho^0K^+)\gamma)=6.48^{+1.98+1.03}_{-1.55-1.34}\times10^{-6}, \quad (37)$$

and predicting

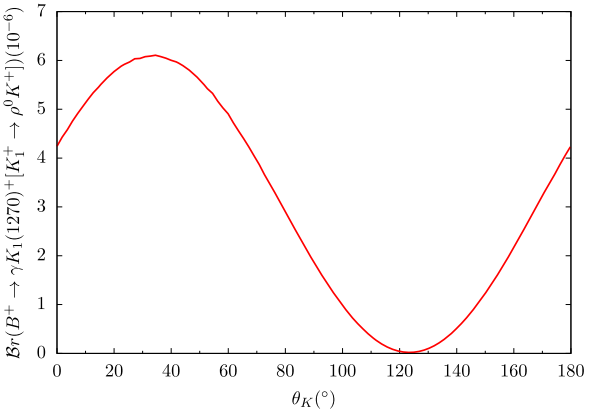

FIG. 1. θ_K dependence of the $B^+\to K_1(1270)(\to\rho^0K^+)\gamma$ branching ratio.

$$\mathcal{B}(B^0\to K_1(1270^0)(\to\rho^0K^0)\gamma)=4.92^{+1.68+0.64}_{-1.24-1.09}\times10^{-6},$$
$$\mathcal{B}(B^0\to K^*(1680^0)(\to\rho^0K^0)\gamma)=5.84^{+1.86+0.96}_{-1.45-1.27}\times10^{-6}. \quad (38)$$

We mention that an upper bound $\omega\le1.8$ GeV for the ρK invariant mass, the same as the experimental cutoff [34], has been applied to the calculation. To test the sensitivity of the branching ratios to the mixing angle θ_K, we fix $c=2.0$, and display the θ_K dependence of the $B^+\to K_1(1270^+)\times(\to\rho^0K^+)\gamma$ branching ratio in Fig. 1. The coordinates $\theta_K\sim33°$ and $58°$ happen to locate on the two sides of a peak, explaining why the results in Eqs. (35) and (37) are close to each other.

Summing the contributions from the two quasi-two-body modes according to Eq. (25), we get

$$\mathcal{B}(B^+\to\rho^0K^+\gamma)=\begin{cases}12.8^{+1.8}_{-2.9}\times10^{-6}, & \text{for } \theta_K=33°,\\ 12.4^{+3.0}_{-2.8}\times10^{-6}, & \text{for } \theta_K=58°,\end{cases} \quad (39)$$

$$\mathcal{B}(B^0\to\rho^0K^0\gamma)=\begin{cases}11.1^{+2.9}_{-2.7}\times10^{-6}, & \text{for } \theta_K=33°,\\ 10.8^{+2.8}_{-2.5}\times10^{-6}, & \text{for } \theta_K=58°,\end{cases} \quad (40)$$

whose theoretical uncertainties contain only those associated with the considered resonances. The isospin symmetry then gives the estimate

$$\mathcal{B}(B^+\to\rho^+K^0\gamma)=2\mathcal{B}(B^+\to\rho^0K^+\gamma),$$
$$\mathcal{B}(B^0\to\rho^-K^+\gamma)=2\mathcal{B}(B^0\to\rho^0K^0\gamma). \quad (41)$$

The direct CP asymmetry in the $B\to PV\gamma$ decay is define by

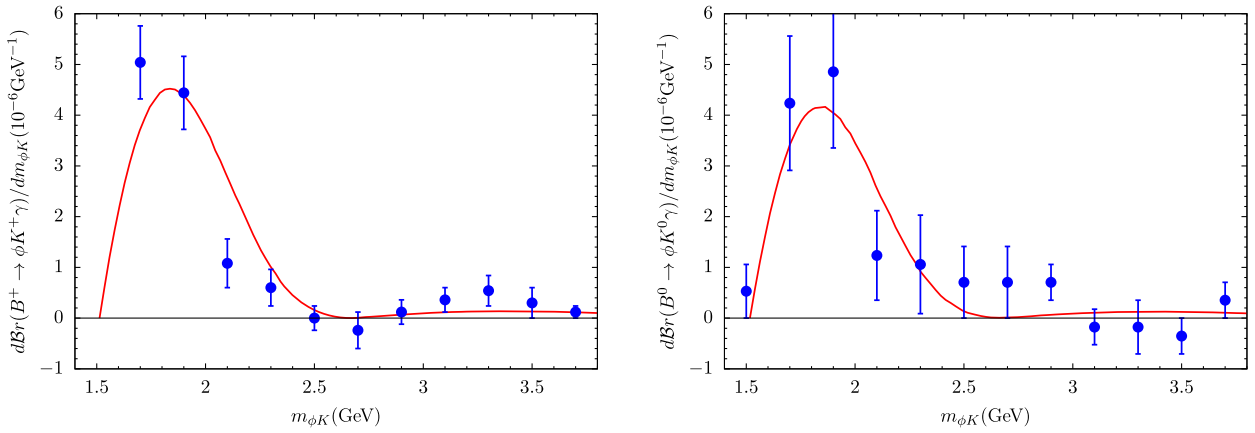

(a) $B^+ \to \phi K^+\gamma$ (b) $B^0 \to \phi K^0\gamma$

FIG. 2. Predicted $B \to \phi K\gamma$ decay spectra (curves) and the Belle data (points with error bars) in the ϕK invariant mass.

$$A_{CP} = \frac{\mathcal{B}(\bar{B} \to \bar{P}\,\bar{V}\,\gamma) - \mathcal{B}(B \to PV\gamma)}{\mathcal{B}(\bar{B} \to \bar{P}\,\bar{V}\,\gamma) + \mathcal{B}(B \to PV\gamma)}. \tag{42}$$

Since the difference of the weak phases between $V_{tb}^* V_{ts}$ and $V_{cb}^* V_{cs}$ is negligible, the dominant $O_{7\gamma}$ contribution can induce an appreciable CP asymmetry only through its interference with the amplitudes proportional to $V_{ub}^* V_{us}$. We predict the direct CP asymmetries (in units of percentage)

$$A_{CP}(B^+ \to \phi K^+\gamma) = -3.78^{+0.2+0.7}_{-0.1-0.3}, \tag{43}$$

$$A_{CP}(B^0 \to \phi K^0\gamma) = -0.13^{+0.01+0.02}_{-0.01-0.03}, \tag{44}$$

$$A_{CP}(B^+ \to \rho^0 K^+\gamma) = \begin{cases} -2.6^{+0.1+0.2}_{-0.1-0.2}, & \text{for } \theta_K = 33°, \\ -2.7^{+0.1+0.2}_{-0.1-0.2}, & \text{for } \theta_K = 58°, \end{cases} \tag{45}$$

$$A_{CP}(B^0 \to \rho^0 K^0\gamma) = \begin{cases} -0.16^{+0.00+0.04}_{-0.00-0.05}, & \text{for } \theta_K = 33°, \\ -0.14^{+0.00+0.04}_{-0.00-0.05}, & \text{for } \theta_K = 58°, \end{cases} \tag{46}$$

whose errors are smaller than those of the branching fractions, due to the cancellation of partial theoretical uncertainties in the ratio in Eq. (42). If other sources of uncertainties are included, which do not cancel in the ratio, such as the one from the u-quark loop formed by the O_2 operator [46], the errors are expected to become sizable. Both the Belle and *BABAR* Collaborations have measured the direct CP asymmetries (in units of percentage) [29,31]

$$A_{CP}(B^+ \to \phi K^+\gamma) = \begin{cases} -3 \pm 11 \pm 8, & \text{(Belle)}, \\ -26 \pm 14 \pm 5, & \text{(}BABAR\text{)}, \end{cases} \tag{47}$$

which are consistent with our prediction in Eq. (43).

The photon polarization involved in radiative B meson decays has attracted a lot of attentions [30,61–63], whose measurements provide a crucial test for the standard model. In this work we calculate the photon polarization asymmetry defined by [62]

$$P_\gamma = \frac{|\mathcal{A}(B \to PV\gamma_R)|^2 - |\mathcal{A}(B \to PV\gamma_L)|^2}{|\mathcal{A}(B \to PV\gamma_R)|^2 + |\mathcal{A}(B \to PV\gamma_L)|^2}, \tag{48}$$

and find $P_\gamma \simeq 1$, implying that the left-handed contribution is tiny in both the $B \to \phi K\gamma$ and $B \to \rho K\gamma$ modes. This result is equivalent to the dominance of the $O_{7\gamma}$ operator in both the nonresonant and resonant channels. The smallness of the O_{8g}, O_2 and annihilation contributions agrees with the observation made in Ref. [64].

At last, Fig. 2 shows our predictions for the ϕK mass distributions in the $B \to \phi K\gamma$ decays, in which the points with error bars represent the Belle data [29] normalized to the central values $\mathcal{B}(B^+ \to \phi K^+\gamma) = 2.48 \times 10^{-6}$ and $\mathcal{B}(B^0 \to \phi K^0\gamma) = 2.74 \times 10^{-6}$. The comparison manifests the consistency with the Belle measurements: both the predicted and observed $B^+ \to \phi K^+\gamma$ spectra reach the maximum at around $m_{\phi K} \sim 1.8$ GeV after a leap from the threshold. The peak position accords the qualitative argument in the PQCD approach [15] that the dominant nonresonant contributions to three-body B meson decays arise from the region with the invariant mass about $O(\bar{\Lambda} m_B)$, $\bar{\Lambda} = m_B - m_b$ being the B meson and b quark mass difference. The predicted $B \to \rho K\gamma$ decay spectra, presented in Fig. 3, exhibit two peaks around the $K_1(1270)$ and $K^*(1680)$ masses as expected. Our predictions for the above decay spectra can be confronted with future data.

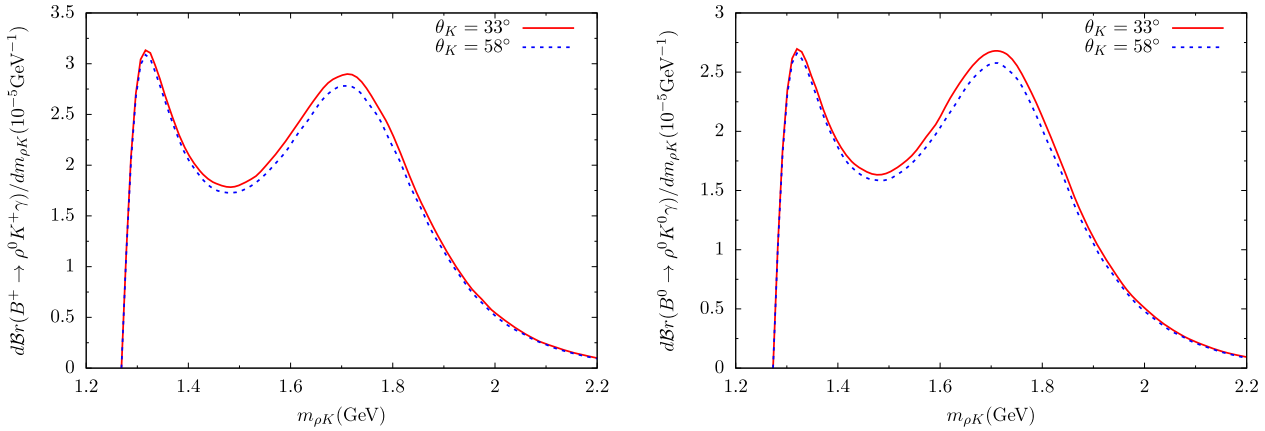

(a) $B^+ \to \rho^+ K^0\gamma$ (b) $B^0 \to \rho^- K^+\gamma$

FIG. 3. Predicted $B \to \rho K\gamma$ decay spectra in the ρK invariant mass with the K_1 mixing angle $\theta_K = 33°(c = 2.0)$ and $58°(c = 1.8)$.

IV. SUMMARY

In this paper we have explored the three-body radiative decays $B \to PV\gamma$ in the PQCD framework, concentrating on the $B \to \phi(\rho)K\gamma$ modes. The dominant contributions to three-body B meson decays originate from the regions corresponding to edges of Dalitz plots, where two final state mesons are nearly collimated with each other. The PV DAs have been introduced to absorb the infrared dynamics in the meson pair, so that a three-body decay amplitude can be factorized, similar to the two-body case, into the convolution of the PV DAs and hard kernels. We have extracted the dependence of the PV DAs on the meson momentum fraction through their normalizations to the time-like form factors, and proposed appropriate parametrizations for the nonsonant and resonant contributions. For the $B \to \phi K\gamma$ decays, the nonresonant contributions dominate, and the prominent feature of the decay spectra is the enhancement near the threshold. For the $B \to \rho K\gamma$ decays, we have adopted the Breit-Wigner model with a tunable parameter to characterize the relative strength between the $K_1(1270)$ and $K^*(1680)$ states.

Fitting the PQCD factorization formulas to the branching-ratio data, we have fixed the free parameters in the PV DAs, which were then employed to predict the direct CP asymmetries, the decay spectra and the photon polarization asymmetries of the $B \to \phi(\rho)K\gamma$ modes. The $O_{7\gamma}$, O_{8g}, and O_2 operators, and the annihilation contributions have been taken into account, so this work is more complete than in the literature [32], where only the emission diagrams from $O_{7\gamma}$ were considered. It has been shown that our results are in good agreement with all the existing data. More precise data from future experiments will help testing our predictions, including other minor resonances which have been ignored here, and improving the application of the PQCD formalism to more three-body B meson decays.

The analysis of the $B \to K^*\pi\gamma$ decays is similar, but requires the inclusion of all the $K_1(1270)$, $K_1(1400)$, $K^*(1410)$, and $K^*(1680)$ intermediate states [34]. Five parameters are then needed to describe the interference among the resonances with the same spin parity, three of them accounting for the magnitudes and two for the phases. The present data are not sufficient to determine these parameters, so we will leave the $B \to K^*\pi\gamma$ modes to a future investigation.

ACKNOWLEDGMENTS

We thank W.-F. Wang and W. Wang for useful discussions. This work was supported in part by the Ministry of Science and Technology of R. O. C. under Grant No. MOST-104-2112-M-001-037-MY3, and by National Natural Science Foundation of China under Grants No. 11575151, No. 11375208, No. 11521505, No. 11621131001, and No. 11235005.

APPENDIX: FACTORIZATION FORMULAS

The effective Hamiltonian relevant to the $b \to s$ transition is given by [65]

$$H_{\mathrm{eff}} = \frac{G_F}{\sqrt{2}}\left[\sum_{q=u,c} V_{qb}V_{qs}^*\{C_1(\mu)O_1^{(q)}(\mu) + C_2(\mu)O_2^{(q)}(\mu)\} - V_{tb}V_{ts}^*\sum_{i=3\sim 8g} C_i(\mu)O_i(\mu)\right] + \mathrm{H.c.}, \tag{A1}$$

with the Wilson coefficients C_i and the local operators

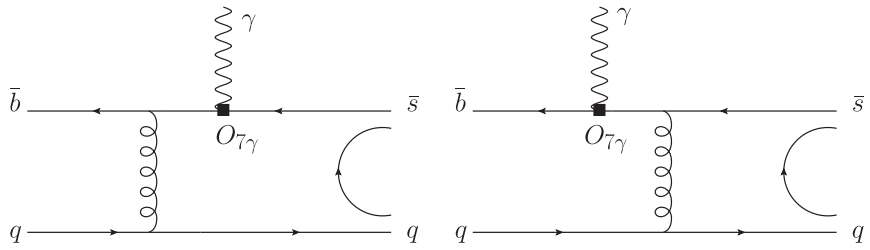

FIG. 4. Feynman diagrams from the operator $O_{7\gamma}$.

$$O_1^{(q)} = (\bar{s}_i q_j)_{V-A}(\bar{q}_j b_i)_{V-A}, \qquad O_2^{(q)} = (\bar{s}_i q_i)_{V-A}(\bar{q}_j b_j)_{V-A}, \qquad O_3 = (\bar{s}_i b_i)_{V-A}\sum_q (\bar{q}_j q_j)_{V-A},$$
$$O_4 = (\bar{s}_i b_j)_{V-A}\sum_q (\bar{q}_j q_i)_{V-A}, \qquad O_5 = (\bar{s}_i b_i)_{V-A}\sum_q (\bar{q}_j q_j)_{V+A}, \qquad O_6 = (\bar{s}_i b_j)_{V-A}\sum_q (\bar{q}_j q_i)_{V+A},$$
$$O_{7\gamma} = \frac{e}{8\pi^2} m_b \bar{s}_i \sigma^{\mu\nu}(1+\gamma_5) b_i F_{\mu\nu}, \qquad O_{8g} = \frac{g}{8\pi^2} m_b \bar{s}_i \sigma^{\mu\nu}(1+\gamma_5) T^a_{ij} b_j G^a_{\mu\nu}, \tag{A2}$$

where the terms associated with the strange quark mass in the $O_{7\gamma}$ and O_{8g} operators have been dropped.

The dominant contributions to the three-body radiative decays $B \to PV\gamma$ come from $O_{7\gamma}$, whose diagrams are displayed in Fig. 4 with the photon being emitted from the operator. The factorization formulas for the emissions of the right-handed and left-handed photons are written as

$$\mathcal{M}^R_{7\gamma} = -4C_F \frac{e}{\pi} m_b m_B^4 \int_0^1 dx_1 dz \int_0^\infty b_1 db_1 b_2 db_2 \phi_B(x_1, b_1)(1-\eta)\{[(1+z)\phi_t \tag{A3}$$
$$+ \sqrt{\eta}(1-2z)(\phi_v + \phi_a)]E_e(t_a) h_a(x_1, z, b_1, b_2) + \sqrt{\eta}(\phi_v + \phi_a) E_e(t'_a) h'_a(x_1, z, b_1, b_2)\},$$
$$\mathcal{M}^L_{7\gamma} = 0, \tag{A4}$$

respectively, where the left-helicity amplitude $\mathcal{M}^L_{7\gamma}$ vanishes because of the neglect of the strange quark mass, and the arguments z, ζ, and ω of the PV DAs are implicit.

The diagrams associated with the operator O_{8g} are depicted in Fig. 5, where the hard gluon from the operator O_{8g} kicks the soft spectator, making it an energetic collinear quark, and the photon is emitted via the bremsstrahlung. The amplitudes are written as

$$\mathcal{M}^{R(a)}_{8g} = \frac{2C_F}{\pi} m_b m_B^4 e \int_0^1 dx_1 dz \int_0^\infty b_1 db_1 b_2 db_2 \phi_B(x_1, b_1)\{[(x_1 - 2z)\phi_t + 3\sqrt{\eta} z(\phi_v + \phi_a)]Q_s E_e(t_b)$$
$$\times h_b(x_1, z, b_1, b_2) - [(1 - \eta + x_1)(x_1\phi_t + \sqrt{\eta} z(\phi_v + \phi_a))]Q_b E_e(t'_b) h'_b(x_1, z, b_1, b_2)\}, \tag{A5}$$

$$\mathcal{M}^{L(a)}_{8g} = \frac{2C_F}{\pi} m_b m_B^4 Q_s e \int_0^1 dx_1 dz \int_0^\infty b_1 db_1 b_2 db_2 \phi_B(x_1, b_1)\{(1-z)(\eta(2x_1 - z)\phi_t$$
$$+ 3x_1\sqrt{\eta}(\phi_v - \phi_a))\} E_e(t_b) h_b(x_1, z, b_1, b_2), \tag{A6}$$

for the first two diagrams, where $Q_{b(s)}$ labels the charge of the b (s) quark in units of the electron charge e, and as

$$\mathcal{M}^{R(b)}_{8g}(Q_q) = \frac{2C_F}{\pi} m_b m_B^4 Q_q e \int_0^1 dx_1 dz \int_0^\infty b_1 db_1 b_2 db_2 \phi_B(x_1, b_1)\{-(1-\eta)[(2 + z - 2\eta - x_1)\phi_t$$
$$+ 3\sqrt{\eta} z(\phi_v + \phi_a)]E_e(t_c) h_c(x_1, z, b_1, b_2) + [(1-\eta)(x_1\phi_t + \sqrt{\eta}(x_1 - z)(\phi_v + \phi_a))]$$
$$\times E_e(t'_c) h'_c(x_1, z, b_1, b_2)\}, \tag{A7}$$

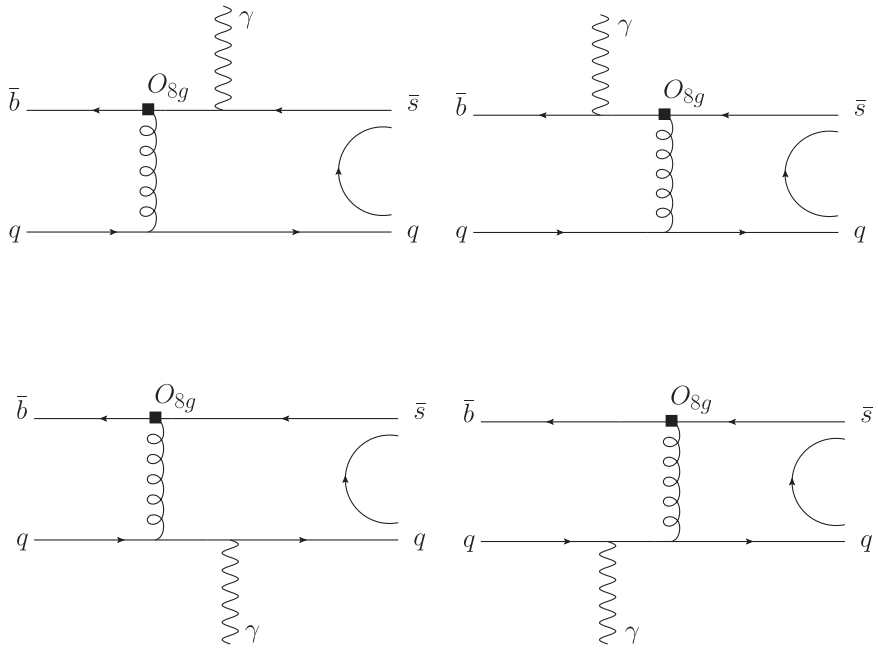

FIG. 5. Feynman diagrams from the operator O_{8g}.

$$\mathcal{M}_{8g}^{L(b)}(Q_q) = \frac{2C_F}{\pi} m_b m_B^4 Q_q e \int_0^1 dx_1 dz \int_0^\infty b_1 db_1 b_2 db_2 \phi_B(x_1, b_1)\{[-z\eta(1+2z-2x_1-\eta)\phi_t + 3\sqrt{\eta}(1-\eta)(z-x_1)(\phi_v-\phi_a)]E_e(t_c)h_c(x_1,z,b_1,b_2) + [(1-\eta)(\eta(x_1-z)\phi_t - \sqrt{\eta}x_1(\phi_v-\phi_a))]E_e(t_c')h_c'(x_1,z,b_1,b_2)\}, \tag{A8}$$

for the last two diagrams.

Next we consider the quark loop corrections from the operators O_i. The operator O_1 does not contribute due to the color mismatch, and the $O_{3\text{–}6}$ insertions are small compared to the O_2 insertion. Hence, we concentrate only on the O_2 contributions, in which the photon is emitted either by an external quark or from the quark loop.

The diagrams with the photon being emitted by an external quark are shown in Fig. 6. The effective vertex $\bar{b} \to \bar{s}g$ resulting from the loop integration in the $\overline{\text{MS}}$ scheme is given by [66]

$$I^\nu = -\frac{g}{8\pi^2}\left[G(m_i^2,k^2,\mu) - \frac{2}{3}\right]\bar{b}T^a(k^2\gamma^\nu - k^\nu \not{k})(1-\gamma_5)s,$$
$$G(m_i^2,k^2,\mu) = -\int_0^1 dx 4x(1-x)\log\left[\frac{m_i^2 - x(1-x)k^2 - i\epsilon}{\mu^2}\right], \tag{A9}$$

where k is the virtual gluon momentum and m_i, $i = u$, c, are the masses of the quarks in the loop. The amplitudes are written as

$$\mathcal{M}_{1i}^{R(a)} = \frac{C_F}{\pi} m_B^5 Q_s e \int_0^1 dx_1 dz \int_0^\infty b_1 db_1 b_2 db_2 \phi_B(x_1,b_1)\left[G(m_i^2, -x_1 z m_B^2, t_b) - \frac{2}{3}\right] \times z(3x_1\phi_t + \sqrt{\eta}(z-2x_1)(\phi_v+\phi_a))E_e(t_b)h_b(x_1,z,b_1,b_2), \tag{A10}$$

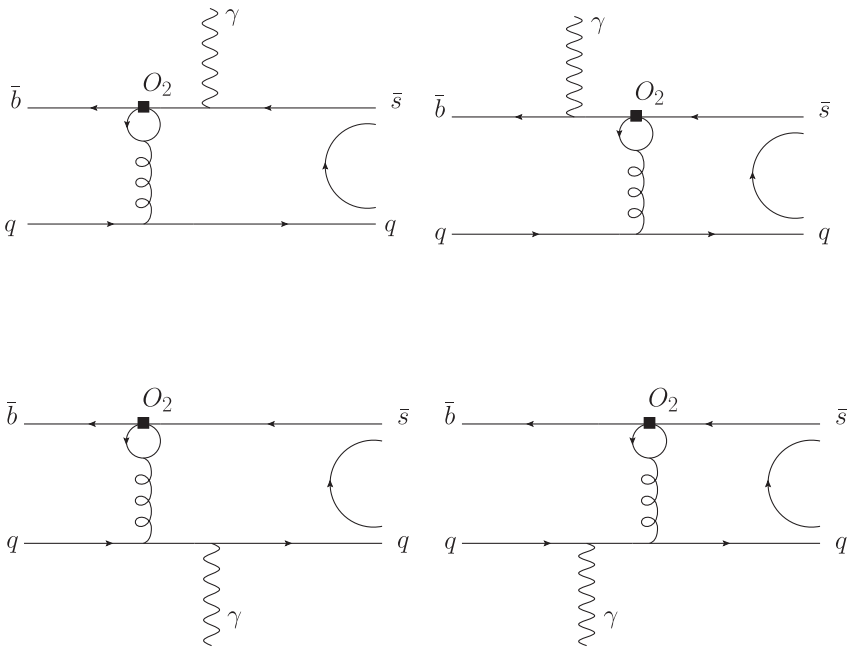

FIG. 6. Quark-loop diagrams from the operator O_2 with a photon being emitted by an external quark.

$$\mathcal{M}_{1i}^{L(a)} = \frac{C_F}{\pi} m_B^5 e \int_0^1 dx_1 dz \int_0^\infty b_1 db_1 b_2 db_2 \phi_B(x_1, b_1) \Bigg\{ \left[G(m_i^2, -x_1 z m_B^2, t_b) - \frac{2}{3} \right] x_1 (1-z) \times (3\eta z \phi_t + \sqrt{\eta}(2z - x_1)(\phi_v - \phi_a)) Q_s E_e(t_b) h_b(x_1, z, b_1, b_2) - \left[G(m_i^2, -x_1 z m_B^2, t_b') - \frac{2}{3} \right] (z(1 - \eta + x_1)(\eta z \phi_t - x_1 \sqrt{\eta}(\phi_v - \phi_a))) Q_b E_e(t_b') h_b'(x_1, z, b_1, b_2) \Bigg\}, \tag{A11}$$

for the first two diagrams, and as

$$\mathcal{M}_{1i}^{R(b)}(Q_q) = -\frac{C_F}{\pi} m_B^5 Q_q e \int_0^1 dx_1 dz \int_0^\infty b_1 db_1 b_2 db_2 \phi_B(x_1, b_1) \Bigg\{ \left[G(m_i^2, (z - x_1)(1-\eta) m_B^2, t_c) - \frac{2}{3} \right] (1-\eta)[3(z - x_1)(1-\eta)\phi_t + z\sqrt{\eta}(1 + 2z - \eta - 2x_1)(\phi_v + \phi_a)] E_e(t_c) h_c(x_1, z, b_1, b_2) - \left[G(m_i^2, (z - x_1)(1-\eta) m_B^2, t_c') - \frac{2}{3} \right] ((1-\eta)^2 (x_1 \phi_t + \sqrt{\eta}(x_1 - z)(\phi_v + \phi_a))) \times E_e(t_c') h_c'(x_1, z, b_1, b_2) \Bigg\}, \tag{A12}$$

$$\mathcal{M}_{1i}^{L(b)}(Q_q) = -\frac{C_F}{\pi} m_B^5 Q_q e \int_0^1 dx_1 dz \int_0^\infty b_1 db_1 b_2 db_2 \phi_B(x_1, b_1) \Bigg\{ \left[G(m_i^2, (z - x_1)(1-\eta) m_B^2, t_c) - \frac{2}{3} \right] (1-\eta)(z - x_1)[3\eta z \phi_t - \sqrt{\eta}(2 + z - 2\eta - x_1)(\phi_v - \phi_a)] E_e(t_c) h_c(x_1, z, b_1, b_2) + \left[G(m_i^2, (z - x_1)(1-\eta) m_B^2, t_c') - \frac{2}{3} \right] [(1-\eta)(x_1 - z)(\eta(x_1 - z)\phi_t - \sqrt{\eta} x_1 (\phi_v - \phi_a))] \times E_e(t_c') h_c'(x_1, z, b_1, b_2) \Bigg\}, \tag{A13}$$

for the last two diagrams.

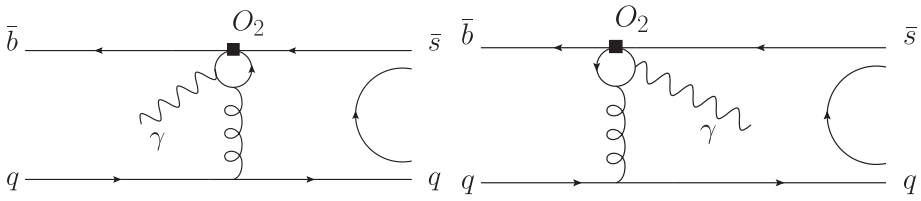

FIG. 7. Quark-loop diagrams from the operator O_2 with the photon being emitted from the quark loop.

In the case where the photon is emitted from the quark loop, as displayed in Fig. 7, the sum of the effective vertex $\bar{b} \to \bar{s}\gamma g^*$ produces [67,68]

$$I = \bar{b}\gamma^\rho \frac{(1-\gamma_5)}{2} T^a s I_{\mu\nu\rho} A^\mu A^{a\nu}, \tag{A14}$$

where

$$I_{\mu\nu\rho} = A_4[(q\cdot k)\epsilon_{\mu\nu\rho\sigma}(q-k)^\sigma + \epsilon_{\nu\rho\sigma\tau}q^\sigma k^\tau k_\mu - \epsilon_{\mu\nu\sigma\tau}q^\sigma k^\tau q_\nu] + A_5[\epsilon_{\mu\rho\sigma\tau}q^\sigma k^\tau k_\nu - k^2\epsilon_{\mu\nu\rho\sigma}q^\tau], \tag{A15}$$

with

$$A_4 = -\frac{4ieg}{3\pi^2}\int_0^1 dx \int_0^{1-x} dy \frac{xy}{x(1-x)k^2 + 2xyq\cdot k - m_i^2}, \tag{A16}$$

$$A_5 = \frac{4ieg}{3\pi^2}\int_0^1 dx \int_0^{1-x} dy \frac{x(1-x)}{x(1-x)k^2 + 2xyq\cdot k - m_i^2}, \tag{A17}$$

q (k) being the photon (gluon) momentum. The amplitudes for the two diagrams are expressed as

$$\begin{aligned}\mathcal{M}_{2i}^R = &-\frac{8}{3}\frac{C_F}{\pi}m_B^5 e\int_0^1 dx\int_0^{1-x} dy\int_0^1 dx_1 dz\int_0^\infty b_1 db_1 \phi_B(x_1,b_1)\alpha_s(t_d)e^{-S_B(t_d)}\\ &\times\frac{h'_e}{xyz(1-\eta)m_B^2 - m_i^2}\times(1-\eta)z\{xy[(1-\eta+2x_1)\phi_t - \sqrt{\eta}(1-\eta-z+x_1)(\phi_v+\phi_a)]\\ &- x(1-x)[3x_1\phi_t + \sqrt{\eta}(z-2x_1)(\phi_v+\phi_a)]\},\end{aligned} \tag{A18}$$

$$\begin{aligned}\mathcal{M}_{2i}^L = &\frac{8}{3}\frac{C_F}{\pi}m_B^5 e\int_0^1 dx\int_0^{1-x} dy\int_0^1 dx_1 dz\int_0^\infty b_1 db_1 \phi_B(x_1,b_1)\alpha_s(t_d)e^{-S_B(t_d)}\\ &\times\frac{h'_e}{xyz(1-\eta)m_B^2 - m_i^2}\times(1-\eta)z\{xy[2\eta z\phi_t + (z-x_1)\sqrt{\eta}(\phi_v-\phi_a)] - x(1-x)\\ &\times[\eta z\phi_t - x_1\sqrt{\eta}(\phi_v-\phi_a)]\},\end{aligned} \tag{A19}$$

in which the function h'_e is defined by

$$h'_e = K_0(\sqrt{x_1 z}m_B b_1) - \left[\theta(B^2)K_0(b_1\sqrt{B^2}) + \theta(-B^2)\frac{i\pi}{2}H_0^{(1)}(b_1\sqrt{|B^2|})\right], \tag{A20}$$

with

$$B^2 = x_1 z m_B^2 - \frac{yz(1-\eta)}{1-x}m_B^2 + \frac{m_i^2}{x(1-x)}. \tag{A21}$$

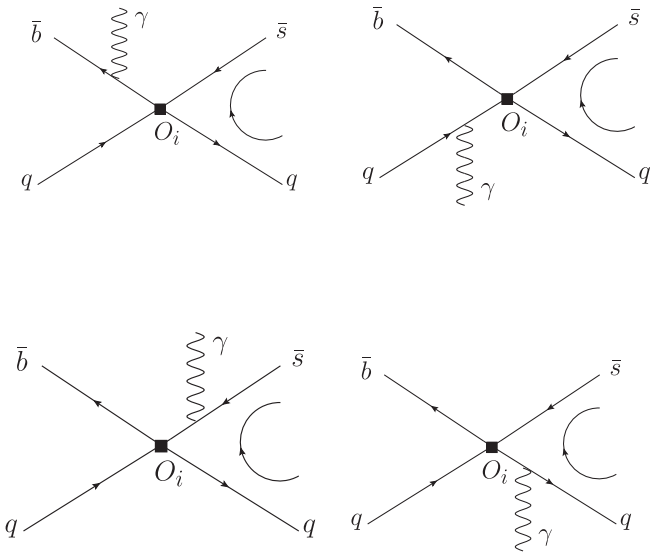

FIG. 8. Annihilation diagrams.

The annihilation diagrams are exhibited in Fig. 8, to which three types of operators contribute, the left-handed current between the $\bar{b}$ and q quarks and the left-handed current between the final state quarks (LL); the left-handed current between the $\bar{b}$ and q quarks and the right-handed current between the final state quarks (LR); the $(S-P)(S+P)$ current from the Fierz transformation of the $(V-A)(V+A)$ operators (SP). Here we define the combinations of the Wilson coefficients,

$$\begin{aligned} a_1 &= C_2 + C_1/3, \qquad a_4 = C_4 + C_3/3, \\ a_6 &= C_6 + C_5/3, \qquad a_8 = C_8 + C_7/3, \\ a_{10} &= C_{10} + C_9/3. \end{aligned} \tag{A22}$$

The factorization formulas for the annihilation contributions are given by

$$\mathcal{M}_{ann}^{R(a,LL)}(Q_q) = 2\sqrt{6\eta}m_B^3 Q_q e[(2\zeta-1)F_v + F_a]\int_0^1 dx \int_0^\infty b_1 db_1 \phi_B(x_1,b_1) \times E_a(t_e') K_0(\sqrt{x_1(1-\eta)}m_B b_1)(1-\eta), \tag{A23}$$

$$\begin{aligned} \mathcal{M}_{ann}^{L(a,LL)}(Q_q) = 2\sqrt{6\eta}m_B^3 e[(2\zeta-1)F_v - F_a)\int_0^1 dx \int_0^\infty b_1 db_1 \phi_B(x_1,b_1) \\ \times \{Q_b E_a(t_e) K_0(\sqrt{1-\eta+x_1}m_B b_1)(1-\eta+x_1) + Q_q E_a(t_e') K_0(\sqrt{x_1(1-\eta)}m_B b_1)x_1\}, \end{aligned} \tag{A24}$$

$$\mathcal{M}_{ann}^{R(a,LR)}(Q_q) = 2\sqrt{6\eta}m_B^3 Q_q e[(2\zeta-1)F_v - F_a]\int_0^1 dx \int_0^\infty b_1 db_1 \phi_B(x_1,b_1) \times E_a(t_e') K_0(\sqrt{x_1(1-\eta)}m_B b_1)(1-\eta), \tag{A25}$$

$$\begin{aligned} \mathcal{M}_{ann}^{L(a,LR)}(Q_q) = 2\sqrt{6\eta}m_B^3 e[(2\zeta-1)F_v + F_a)\int_0^1 dx \int_0^\infty b_1 db_1 \phi_B(x_1,b_1) \\ \times \{Q_b E_a(t_e) K_0(\sqrt{1-\eta+x_1}m_B b_1)(1-\eta+x_1) + Q_q E_a(t_e') K_0(\sqrt{x_1(1-\eta)}m_B b_1)x_1\}, \end{aligned} \tag{A26}$$

$$\begin{aligned} \mathcal{M}_{ann}^{R(b,LL)}(Q_q) &= -\mathcal{M}_{ann}^{L,(b,LR)}(Q_q) \\ &= -2\sqrt{6\eta}ef_B m_B^3 \int_0^1 dz \int_0^\infty b_2 db_2 \Big\{ Q_s(\phi_v+\phi_a)E_a'(t_f)\frac{i\pi}{2}H_0^{(1)}(\sqrt{1-z}m_B b_2) \\ &\quad - Q_q z(\phi_v+\phi_a)E_a'(t_f')\frac{i\pi}{2}H_0^{(1)}(\sqrt{z(1-\eta)}m_B b_2)\Big\}, \end{aligned} \tag{A27}$$

$$\begin{aligned} \mathcal{M}_{ann}^{L(b,LL)}(Q_q) &= -\mathcal{M}_{ann}^{R,(b,LR)}(Q_q) \\ &= 2\sqrt{6\eta}ef_B m_B^3 \int_0^1 dz \int_0^\infty b_2 db_2 \Big\{ Q_s(1-z)(\phi_v-\phi_a)E_a'(t_f)\frac{i\pi}{2}H_0^{(1)}(\sqrt{1-z}m_B b_2) \\ &\quad - (1-\eta)Q_q(\phi_v-\phi_a)E_a'(t_f')\frac{i\pi}{2}H_0^{(1)}(\sqrt{z(1-\eta)}m_B b_2)\Big\}, \end{aligned} \tag{A28}$$

$$\mathcal{M}_{ann}^{R(SP)}(Q_q) = 4\sqrt{6}ef_B m_B^3 \int_0^1 dz \int_0^\infty b_2 db_2 \Big\{ Q_s \phi_t E_a'(t_f) \frac{i\pi}{2} H_0^{(1)}(\sqrt{1-z} m_B b_2) + Q_q(1-\eta)\phi_t E_a'(t_f') \frac{i\pi}{2} H_0^{(1)}(\sqrt{z(1-\eta)} m_B b_2) \Big\}, \tag{A29}$$

$$\mathcal{M}_{ann}^{L(SP)}(Q_q) = 4\sqrt{6}ef_B m_B^3 \int_0^1 dz \int_0^\infty b_2 db_2 \Big\{ Q_s \eta(1-z)\phi_t E_a'(t_f) \frac{i\pi}{2} H_0^{(1)}(\sqrt{1-z} m_B b_2) + Q_q \eta z \phi_t E_a'(t_f') \frac{i\pi}{2} H_0^{(1)}(\sqrt{z(1-\eta)} m_B b_2) \Big\}. \tag{A30}$$

Finally, we sum the squared amplitudes for the B^+ meson decays in the helicity basis, $|\mathcal{A}(B^+)|^2 = \sum_{i=R,L} |\mathcal{A}^i(B^+)|^2$, with

$$\begin{aligned}\mathcal{A}^i(B^+) = {} & \frac{G_F}{\sqrt{2}} V_{ub}^* V_{us} \{ C_2(\mathcal{M}_{1u}^{i(a)} + \mathcal{M}_{1u}^{i(b)}(Q_u) + \mathcal{M}_{2u}^i) + a_1(\mathcal{M}_{ann}^{i(a,LL)}(Q_u) + \mathcal{M}_{ann}^{i(b,LL)}(Q_u)) \} \\ & + \frac{G_F}{\sqrt{2}} V_{cb}^* V_{cs} \{ C_2(\mathcal{M}_{1c}^{i(a)} + \mathcal{M}_{1c}^{i(b)}(Q_u) + \mathcal{M}_{2c}^i) \} - \frac{G_F}{\sqrt{2}} V_{tb}^* V_{ts} \{ C_{7\gamma} \mathcal{M}_{7\gamma}^i + C_{8g}(\mathcal{M}_{8g}^{i(a)} + \mathcal{M}_{8g}^{i(b)}(Q_u)) \\ & + (a_4 + a_{10})(\mathcal{M}_{ann}^{i(a,LL)}(Q_u) + \mathcal{M}_{ann}^{i(b,LL)}(Q_u)) + (a_6 + a_8)\mathcal{M}_{ann}^{i(SP)}(Q_u) \}. \end{aligned} \tag{A31}$$

We have the similar sum for the B^0 meson decay amplitudes with

$$\begin{aligned}\mathcal{A}^i(B^0) = {} & \frac{G_F}{\sqrt{2}} V_{ub}^* V_{us} \{ C_2(\mathcal{M}_{1u}^{i(a)} + \mathcal{M}_{1u}^{i(b)}(Q_d) + \mathcal{M}_{2u}^i) \} + \frac{G_F}{\sqrt{2}} V_{cb}^* V_{cs} \{ C_2(\mathcal{M}_{1c}^{i(a)} + \mathcal{M}_{1c}^{i(b)}(Q_d) + \mathcal{M}_{2c}^i) \} \\ & - \frac{G_F}{\sqrt{2}} V_{tb}^* V_{ts} \Big\{ C_{7\gamma} \mathcal{M}_{7\gamma}^i + C_{8g}(\mathcal{M}_{8g}^{i(a)} + \mathcal{M}_{8g}^{i(b)}(Q_d)) \\ & + \Big(a_4 - \frac{1}{2}a_{10}\Big)(\mathcal{M}_{ann}^{i(a,LL)}(Q_d) + \mathcal{M}_{ann}^{i(b,LL)}(Q_d)) + \Big(a_6 - \frac{1}{2}a_8\Big)\mathcal{M}_{ann}^{i(SP)}(Q_d) \Big\}. \end{aligned} \tag{A32}$$

It is seen that the $O_{7\gamma}$ contributions to the B^+ and B^0 meson decays are identical.

The explicit expressions for some functions appearing in the above factorization formulas are presented below. We adopt the model

$$\phi_B(x,b) = N_B x^2(1-x)^2 \exp\left[-\frac{1}{2}\left(\frac{x m_B}{\omega_B}\right)^2 - \frac{1}{2}(\omega_B b)^2 \right], \tag{A33}$$

for the B meson DA, where b is the impact parameter conjugate to the spectator transverse momentum k_T, N_B is the normalization constant, and the shape parameter $\omega_B = 0.40 \pm 0.04$ GeV has been determined through the study of the B meson transition form factors [43,44].

The hard scales are chosen as

$$\begin{aligned} & t_a = \max\{\sqrt{z} m_B, 1/b_1, 1/b_2\}, \qquad t_a' = \max\{\sqrt{|x_1-\eta|} m_B, \sqrt{z x_1} m_B, 1/b_1, 1/b_2\}, \\ & t_b = \max\{\sqrt{1-z} m_B, \sqrt{z x_1} m_B, 1/b_1, 1/b_2\}, \qquad t_b' = \max\{\sqrt{1+x_1-\eta} m_B, \sqrt{z x_1} m_B, 1/b_1, 1/b_2\}, \\ & t_c = \max\{\sqrt{z(1-\eta)} m_B, \sqrt{|(x_1-z)(1-\eta)|} m_B, 1/b_1, 1/b_2\}, \\ & t_c' = \max\{\sqrt{x_1(1-\eta)} m_B, \sqrt{|(x_1-z)(1-\eta)|} m_B, 1/b_1, 1/b_2\}, \\ & t_d = \max\{\sqrt{x_1 z} m_B, \sqrt{|B^2|}, 1/b_1\}, \qquad t_e = \max\{\sqrt{1-\eta+x_1} m_B, 1/b_1\}, \qquad t_e' = \max\{\sqrt{x_1(1-\eta)} m_B, 1/b_1\}, \\ & t_f = \max\{\sqrt{1-z} m_B, 1/b_2\}, \qquad t_f' = \max\{\sqrt{z(1-\eta)} m_B, 1/b_2\}. \end{aligned} \tag{A34}$$

The hard functions are written as

$$
\begin{aligned}
h_a(x_1,z,b_1,b_2) &= K_0(\sqrt{zx_1}m_Bb_1)[\theta(b_1-b_2)K_0(\sqrt{z}m_Bb_1)I_0(\sqrt{z}m_Bb_2)+(b_1\leftrightarrow b_2)]S_t(z),\\
h'_a(x_1,z,b_1,b_2) &= K_0(\sqrt{zx_1}m_Bb_2)S_t(x_1)\\
&\quad\times\begin{cases}\frac{i\pi}{2}[\theta(b_2-b_1)H_0^{(1)}(\sqrt{|x_1-\eta|}m_Bb_2)J_0(\sqrt{|x_1-\eta|}m_Bb_1)+(b_2\leftrightarrow b_1)], & x_1<\eta,\\ \theta(b_2-b_1)K_0(\sqrt{x_1-\eta}m_Bb_2)I_0(\sqrt{x_1-\eta}m_Bb_1)+(b_2\leftrightarrow b_1), & x_1>\eta,\end{cases}\\
h_b(x_1,z,b_1,b_2) &= K_0(\sqrt{x_1z}m_Bb_1)\frac{i\pi}{2}[\theta(b_1-b_2)H_0^{(1)}(\sqrt{1-z}m_Bb_1)J_0(\sqrt{1-z}m_Bb_2)+(b_2\leftrightarrow b_1)]S_t(z),\\
h'_b(x_1,z,b_1,b_2) &= K_0(\sqrt{x_1z}m_Bb_2)S_t(x_1)[\theta(b_2-b_1)K_0(\sqrt{1+x_1-\eta}m_Bb_2)I_0(\sqrt{1+x_1-\eta}m_Bb_1)+(b_2\leftrightarrow b_1)],\\
h_c(x_1,z,b_1,b_2) &= \frac{i\pi}{2}[\theta(b_1-b_2)H_0^{(1)}(\sqrt{z(1-\eta)}m_Bb_1)J_0(\sqrt{z(1-\eta)}m_Bb_2)+(b_2\leftrightarrow b_1)]S_t(z)\\
&\quad\times\begin{cases}\frac{i\pi}{2}H_0^{(1)}(\sqrt{|(x_1-z)(1-\eta)|}m_Bb_1), & x_1<z,\\ K_0(\sqrt{(x_1-z)(1-\eta)}m_Bb_1), & x_1>z,\end{cases}\\
h'_c(x_1,z,b_1,b_2) &= [\theta(b_2-b_1)K_0(\sqrt{x_1(1-\eta)}m_Bb_2)I_0(\sqrt{x_1(1-\eta)}m_Bb_1)+(b_2\leftrightarrow b_1)]S_t(x_1)\\
&\quad\times\begin{cases}\frac{i\pi}{2}H_0^{(1)}(\sqrt{|(x_1-z)(1-\eta)|}m_Bb_2), & x_1<\eta,\\ K_0(\sqrt{(x_1-z)(1-\eta)}m_Bb_2), & x_1>z.\end{cases}
\end{aligned}
$$

The Sudakov factor $S_t(x)$ from the threshold resummation follows the parametrization in [69]

$$S_t(x)=\frac{2^{1+2a}\Gamma(3/2+a)}{\sqrt{\pi}\Gamma(1+a)}[x(1-x)]^a, \tag{A35}$$

with the parameter $a=0.4$. The evolution factors are given by

$$E_e(t)=\alpha_s(t)\exp[-S_B(t)-S_2(t)],\qquad E_a(t)=S_t(x_1)\exp[-S_B(t)],\qquad E'_a(t)=S_t(z)\exp[-S_2(t)], \tag{A36}$$

with the Sudakov exponents

$$S_B(t)=s\left(x_1\frac{m_B}{\sqrt{2}},b_1\right)+\frac{5}{3}\int_{1/b_1}^{t}\frac{d\bar{\mu}}{\bar{\mu}}\gamma_q(\alpha_s(\bar{\mu})),\qquad S_2(t)=s\left(z\frac{m_B}{\sqrt{2}},b_2\right)+s\left((1-z)\frac{m_B}{\sqrt{2}},b_2\right)+2\int_{1/b_2}^{t}\frac{d\bar{\mu}}{\bar{\mu}}\gamma_q(\alpha_s(\bar{\mu})), \tag{A37}$$

$\gamma_q=-\alpha_s/\pi$ being the quark anomalous dimension. The function $s(Q,b)$ is expressed as

$$s(Q,b)=\frac{A^{(1)}}{2\beta_1}\hat{q}\ln\left(\frac{\hat{q}}{\hat{b}}\right)-\frac{A^{(1)}}{2\beta_1}(\hat{q}-\hat{b})+\frac{A^{(2)}}{4\beta_1^2}\hat{q}\ln\left(\frac{\hat{q}}{\hat{b}}-1\right)-\left[\frac{A^{(2)}}{4\beta_1^2}-\frac{A^{(1)}}{4\beta_1}\ln\left(\frac{e^{2\gamma_E-1}}{2}\right)\right]\ln\left(\frac{\hat{q}}{\hat{b}}\right), \tag{A38}$$

where

$$
\begin{aligned}
&\hat{q}=\ln\frac{Q}{\sqrt{2}\Lambda_{\rm QCD}},\qquad \hat{b}=\ln\frac{1}{b\Lambda_{\rm QCD}},\qquad \beta_1=\frac{33-2n_f}{12},\qquad \beta_2=\frac{153-19n_f}{24},\\
&A^{(1)}=\frac{4}{3},\qquad A^{(2)}=\frac{67}{9}-\frac{\pi^2}{3}-\frac{10}{27}n_f+\frac{8}{3}\beta_1\ln\left(\frac{1}{2}e^{\gamma_E}\right),
\end{aligned} \tag{A39}
$$

n_f being the number of the quark flavor, and γ_E the Eular constant.

[1] J. P. Lees *et al.* (*BABAR* Collaboration), Phys. Rev. D **85**, 112010 (2012).
[2] J. P. Lees *et al.* (*BABAR* Collaboration), Phys. Rev. D **85**, 054023 (2012).
[3] B. Aubert *et al.* (*BABAR* Collaboration), Phys. Rev. D **80**, 112001 (2009).
[4] J. P. Lees *et al.* (*BABAR* Collaboration), Phys. Rev. D **83**, 112010 (2011).
[5] B. Aubert *et al.* (*BABAR* Collaboration), Phys. Rev. D **79**, 072006 (2009).
[6] B. Aubert *et al.* (*BABAR* Collaboration), Phys. Rev. D **78**, 012004 (2008).
[7] A. Garmash *et al.* (Belle Collaboration), Phys. Rev. D **71**, 092003 (2005).
[8] A. Garmash *et al.* (Belle Collaboration), Phys. Rev. D **75**, 012006 (2007).
[9] P. Chang *et al.* (Belle Collaboration), Phys. Lett. B **599**, 148 (2004).
[10] A. Garmash *et al.* (Belle Collaboration), Phys. Rev. Lett. **96**, 251803 (2006).
[11] R. Aaij *et al.* (LHCb Collaboration), Phys. Rev. Lett. **111**, 101801 (2013).
[12] R. Aaij *et al.* (LHCb Collaboration), Phys. Rev. Lett. **112**, 011801 (2014).
[13] R. Aaij *et al.* (LHCb Collaboration), Phys. Rev. D **90**, 112004 (2014).
[14] T. Aushev *et al.*, arXiv:1002.5012.
[15] C. H. Chen and H. n. Li, Phys. Lett. B **561**, 258 (2003).
[16] W. F. Wang, H. C. Hu, H. n. Li, and C. D. Lü, Phys. Rev. D **89**, 074031 (2014).
[17] W. F. Wang, H. n. Li, W. Wang, and C. D. Lü, Phys. Rev. D **91**, 094024 (2015).
[18] W. F. Wang and H. n. Li, Phys. Lett. B **763**, 29 (2016).
[19] Z. T. Wei, arXiv:hep-ph/0301174.
[20] B. El-Bennich, A. Furman, R. Kaminski, L. Lesniak, B. Loiseau, and B. Moussallam, Phys. Rev. D **79**, 094005 (2009); **83**, 039903(E) (2011).
[21] S. Krnkl, T. Mannel, and J. Virto, Nucl. Phys. **B899**, 247 (2015).
[22] A. Furman, R. Kaminski, L. Lesniak, and B. Loiseau, Phys. Lett. B **622**, 207 (2005).
[23] H. Y. Cheng and K. C. Yang, Phys. Rev. D **66**, 054015 (2002).
[24] H. Y. Cheng, C. K. Chua, and A. Soni, Phys. Rev. D **76**, 094006 (2007).
[25] M. Diehl, T. Gousset, B. Pire, and O. Teryaev, Phys. Rev. Lett. **81**, 1782 (1998).
[26] M. V. Polyakov, Nucl. Phys. **B555**, 231 (1999).
[27] D. Mller, D. Robaschik, B. Geyer, F.-M. Dittes, and J. Horejsi, Fortschr. Phys. **42**, 101 (1994).
[28] M. Diehl, T. Gousset, and B. Pire, Phys. Rev. D **62**, 073014 (2000).
[29] H. Sahoo *et al.* (Belle Collaboration), Phys. Rev. D **84**, 071101 (2011).
[30] M. Gronau and D. Pirjol, Phys. Rev. D **96**, 013002 (2017).
[31] B. Aubert *et al.* (*BABAR* Collaboration), Phys. Rev. D **75**, 051102 (2007).
[32] C. H. Chen and H. n. Li, Phys. Rev. D **70**, 054006 (2004).
[33] S. Nishida *et al.* (Belle Collaboration), Phys. Rev. Lett. **89**, 231801 (2002).
[34] P. d. A. Sanchez *et al.* (*BABAR* Collaboration), Phys. Rev. D **93**, 052013 (2016).
[35] Y. Li, A. J. Ma, W. F. Wang, and Z. J. Xiao, Phys. Rev. D **95**, 056008 (2017).
[36] A. J. Ma, Y. Li, W. F. Wang, and Z. J. Xiao, Chin. Phys. C **41**, 083105 (2017).
[37] G. P. Lepage and S. J. Brodsky, Phys. Lett. **87B**, 359 (1979).
[38] A. V. Efremov and A. V. Radyushkin, Phys. Lett. **94B**, 245 (1980).
[39] M. Diehl, T. Feldmann, P. Kroll, and C. Vogt, Phys. Rev. D **61**, 074029 (2000).
[40] T. Huang, X. H. Wu, and M. Z. Zhou, Phys. Rev. D **70**, 014013 (2004).
[41] K. C. Yang, Nucl. Phys. **B776**, 187 (2007).
[42] H. Y. Cheng and K. C. Yang, Phys. Rev. D **78**, 094001 (2008); **79**, 039903(E) (2009).
[43] Y. Y. Keum, H. n. Li, and A. I. Sanda, Phys. Lett. B **504**, 6 (2001).
[44] Y. Y. Keum, H. N. Li, and A. I. Sanda, Phys. Rev. D **63**, 054008 (2001).
[45] Y. Y. Keum and H. n. Li, Phys. Rev. D **63**, 074006 (2001).
[46] Y. Y. Keum, M. Matsumori, and A. I. Sanda, Phys. Rev. D **72**, 014013 (2005).
[47] C. D. Lu, M. Matsumori, A. I. Sanda, and M. Z. Yang, Phys. Rev. D **72**, 094005 (2005); **73**, 039902(E) (2006).
[48] W. Wang, R. H. Li, and C. D. Lu, arXiv:0711.0432.
[49] C. Patrignani *et al.* (Particle Data Group Collaboration), Chin. Phys. C **40**, 100001 (2016).
[50] M. Suzuki, Phys. Rev. D **47**, 1252 (1993).
[51] L. Burakovsky and J. T. Goldman, Phys. Rev. D **56**, R1368 (1997).
[52] H. Y. Cheng, Phys. Rev. D **67**, 094007 (2003).
[53] K. C. Yang, Phys. Rev. D **84**, 034035 (2011).
[54] H. Hatanaka and K. C. Yang, Phys. Rev. D **77**, 094023 (2008); **78**, 059902(E) (2008).
[55] A. Tayduganov, E. Kou, and A. L. Yaouanc, Phys. Rev. D **85**, 074011 (2012).
[56] F. Divotgey, L. Olbrich, and F. Giacosa, Eur. Phys. J. A **49**, 135 (2013).
[57] R. J. Dowdall, C. T. H. Davies, R. R. Horgan, C. J. Monahan, and J. Shigemitsu, Phys. Rev. Lett. **110**, 222003 (2013).
[58] F. Bernardoni *et al.* (ALPHA Collaboration), Phys. Lett. B **735**, 349 (2014).
[59] H. K. Sun and M. Z. Yang, Phys. Rev. D **95**, 113001 (2017).
[60] M. J. Baker, J. Bordes, C. A. Dominguez, J. Penarrocha, and K. Schilcher J. High Energy Phys. 07 (2014) 032.
[61] D. Atwood, M. Gronau, and A. Soni, Phys. Rev. Lett. **79**, 185 (1997).
[62] M. Gronau and D. Pirjol, Phys. Rev. D **66**, 054008 (2002).
[63] E. Kou, A. L. Yaouanc, and A. Tayduganov, Phys. Rev. D **83**, 094007 (2011).
[64] M. Matsumori and A. I. Sanda, Phys. Rev. D **73**, 114022 (2006).
[65] G. Buchalla, A. J. Buras, and M. E. Lautenbacher, Rev. Mod. Phys. **68**, 1125 (1996).
[66] M. Bander, D. Silverman, and A. Soni, Phys. Rev. Lett. **43**, 242 (1979).
[67] J. Liu and Y. P. Yao, Phys. Rev. D **42**, 1485 (1990).
[68] H. Simma and D. Wyler, Nucl. Phys. **B344**, 283 (1990).
[69] H. n. Li and K. Ukai, Phys. Lett. B **555**, 197 (2003).